Title
Large Continuous Mechanical Gradient Formation via Metal—Ligand Interactions

Journal
Angewandte Chemie International Edition, 56(49)

ISSN
1433-7851

Authors
Neal, James A
Oldenhuis, Nathan J
Novitsky, Andrea L
et al.

Publication Date
2017-12-04

DOI
10.1002/anie.201707587

Gradient Materials

International Edition: DOI: 10.1002/anie.201707587
German Edition: DOI: 10.1002/ange.201707587

Large Continuous Mechanical Gradient Formation via Metal–Ligand Interactions

*James A. Neal[+], Nathan J. Oldenhuis[+], Andrea L. Novitsky, Emil M. Samson, William J. Thrift, Regina Ragan, and Zhibin Guan**

Abstract: *Mechanical gradients are often employed in nature to prevent biological materials from damage by creating a smooth transition from strong to weak that dissipates large forces. Synthetic mimics of these natural structures are highly desired to improve distribution of stresses at interfaces and reduce contact deformation in manmade materials. Current synthetic gradient materials commonly suffer from non-continuous transitions, relatively small gradients in mechanical properties, and difficult syntheses. Inspired by the polychaete worm jaw, we report a novel approach to generate stiffness gradients in polymeric materials via incorporation of dynamic monodentate metal–ligand crosslinks. Through spatial control of metal ion content, we created a continuous mechanical gradient that spans over a 200-fold difference in stiffness, approaching the mechanical contrast observed in biological gradient materials.*

Materials that provide form and function in living organisms generate and withstand tremendous forces. For example, the club of a peacock mantis shrimp (*Odontodactylus scyllarus*) can experience up to 700 N during a strike.[1] This massive force must be mitigated when transferring between the hard club and soft tissues of the shrimp to prevent serious damage. Cleverly, the dissipation of the large forces is accomplished through a continuous gradient in mechanical properties from hard to soft. Gradients like this allow the forces to be distributed, preventing stress buildup and catastrophic failures in the tissues of living organisms.[2] Synthetic analogs of these natural mechanical gradients have been long pursued to create stronger materials with improved thermal and mechanical stress dissipation as well as fracture toughness at interfaces.[2]

Synthetic mechanical gradients are generally obtained in a layered or lateral orientation. Layered gradients are printed layer-by-layer onto surfaces and are not true continuous gradients due to the segmented fabrication process.[3–5] Some lateral gradients are able to obtain smooth transitions,[6–10] but there are few examples due to the complex synthetic effort required to generate them. Notable examples of previously reported lateral gradients include photoinduced crosslinking of cellulose nanocrystals,[7] ordering of carbon nanotube films,[11] and cellulose nanofibril/polymer nanopapers.[12] While these and other synthetic analogs are functional mechanical gradients,[6,8–10,13–19] they often suffer from relatively small ranges in stiffness (~1 order of magnitude), non-continuous stepwise transitions, and require specialty equipment to fabricate. To improve upon these systems, we sought a synthetic solution that could span a greater range of mechanical properties with a true continuous gradient and facile synthesis. Many examples of gradient materials exist in nature,[20–25] but when searching for routes to gradient formation, the jaw of the polychaete worm became a unique source of inspiration (Figure 1). In contrast to the mineralization and covalent crosslinking used to form many natural gradients,[26–28] the polychaete worm relies on metal–ligand interactions to create a rigid jaw tip to inject venom.[29–31] Specifically, by creating a gradient of zinc or copper through a histidine rich protein network, the increasing number of metal–histidine interactions act as crosslinks and create a mechanical gradient, which can prevent damage to the jaw tip during biting and venom injection.

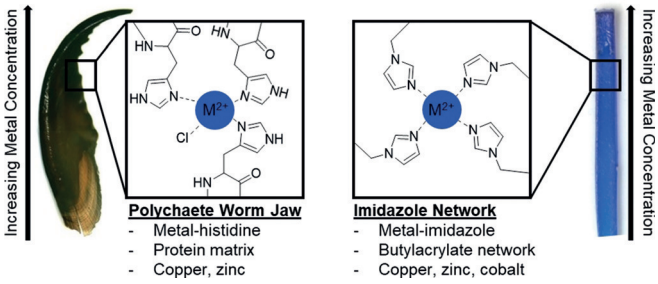

Figure 1. Comparison of the metal–histidine[32] gradient found in the polychaete worm jaw[30] (left) and the metal–imidazole gradient made in this work (right).

In one of our previously reported studies, we investigated control of mechanical properties by altering metal identity (Zn, Cu, Co) and concentration in an imidazole-containing metallopolymer network.[33,34] We employed monodentate imidazole ligands to create dynamic metal–ligand crosslinks. In this past work we found that a weakly binding solvent (acetonitrile, ACN) facilitated ligand exchange (no gelation).

[*] J. A. Neal,[+] Dr. N. J. Oldenhuis,[+] E. M. Samson, Prof. Z. Guan
Department of Chemistry, University of California, Irvine
1102 Natural Sciences 2, Irvine, CA 92697 (USA)
E-mail: zguan@uci.edu
A. L. Novitsky
Nanovea, 6 Morgan Ste 156, Irvine, CA 92618 (USA)
W. J. Thrift, Prof. R. Ragan
Department of Chemical Engineering and Materials Science
University of California, Irvine
Irvine, CA 92697 (USA)
[+] These authors contributed equally to this work.

Supporting information for this article can be found under https://doi.org/10.1002/anie.201707587.

Upon solvent removal the rate of ligand exchange was significantly reduced to create crosslinks that tuned mechanical properties based on metal concentration.

Herein, we leverage our understanding of dynamic imidazole–metal interactions to generate a gradient crosslinked metallopolymer network that exhibits a range of mechanical properties, mimicking the polychaete jaw (Figure 1). To incorporate a gradient of metal into the material, we imagined that we could suspend a polymer sample in a metal salt solution and simultaneously raise it out of the solution, while increasing metal concentration in the reservoir. The dynamic nature of the metal–ligand interaction in the presence of ACN would allow for rapid exchange and metal incorporation into the bulk of the material. Subsequent removal of the solvent would drastically lower the exchange rates of the metal–ligand interactions, resulting in solid materials with stable gradients of metal concentration and mechanical properties (Figure 2).

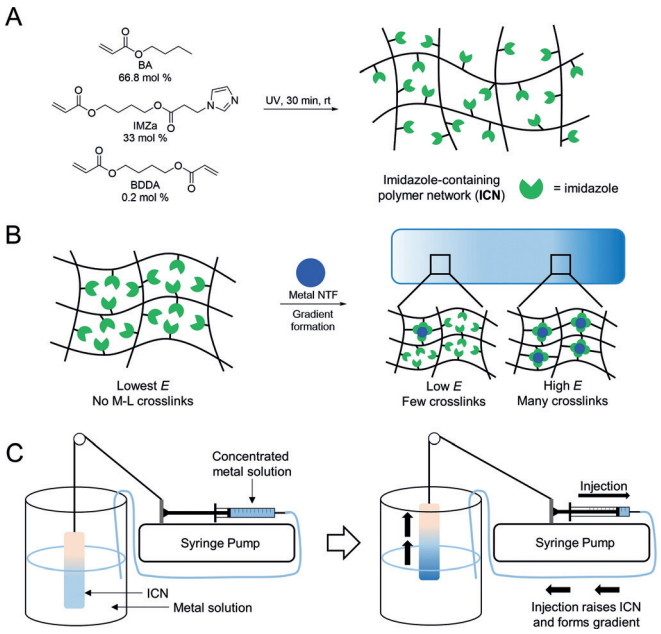

Figure 2. A) Synthesis of the imidazole-containing network (ICN). B) Cartoon depicting metal incorporation into the ICN to form gradient ICN-M. C) Cartoon depicting the use of a common laboratory syringe pump, termed continuous gradient patterner (CGP), to fabricate the gradient sample.

The synthesis of the imidazole-containing network (ICN) is described in Figure 2 A. An imidazole-containing acrylate monomer (IMZa) was copolymerized with butyl acrylate (BA) and 1,4-butanediol diacrylate (BDDA) via UV-initiated polymerization to achieve the ICN. BA was used to lower the glass transition temperature, enhance ligand mobility, and create an initial network with the desired mechanical properties. The BA, IMZa, and BDDA were used in a 66.5:33:0.5 molar ratio, respectively, to achieve the polymer network. The monomer feed ratios were selected based on our previous study, where IMZa incorporation over 35 mol % gave diminished returns of increased mechanical properties.[33] After the synthesis of the ICN, a metal salt (Zn, Cu, or Co) was incorporated via controlled diffusion to form ICN-metal complex (ICN-M). [Bis(trifluoromethylsulfonyl)-imide] (NTF) was selected as the counter ion for all metals due to its well-characterized behaviour, thermal stability, and high mobility in the solid state.

To create the metal gradient in ICN (Figure 2 B), a simple device was designed from a common laboratory syringe pump. The device, termed a continuous gradient patterner (CGP, Figure 2 C) works by first attaching the polymer sample ($3 \times 0.8 \times 25$ mm) via string to the pusher block of the syringe pump and then suspending the sample in a graduated cylinder filled with a stirring solution of metal NTF salt dissolved in ACN. A 1 mL syringe containing a highly concentrated metal NTF salt solution in ACN was adjusted to the length of the sample, such that, while the additional metal solution was being injected into the graduated cylinder, the sample would be slowly raised out of the solution, allowing a gradient to be formed. All ICN-M gradient samples were formed starting with the molar ratio of 0.167 metal atoms per imidazole (i.e., [imidazole]/[metal] = 6.0). During the CGP process, more metal salt was gradually added to finally raise the molar ratio to 0.25 metal atoms per imidazole (i.e., [imidazole]/[metal] = 4.0, details see SI for detailed calculations). These selected values were determined experimentally, as both too much and too little added metal resulted in consistently weaker materials (Figure S2). The syringe pump was set on the lowest flow rate, which typically allowed the polymer sample to raise from the metal solution over 2 days, giving sufficient time for the metal to incorporate into the bulk of the sample. After completion of the CGP process, residual solvent was removed from the crosslinked samples in a vacuum oven.

After metal incorporation and removal of ACN, the bulk mechanical properties of ICN-M samples were studied via indentation using a Nanovea indenter. The Young's modulus (E) and local hardness were calculated based on the single indentation of a spherical tip (radius = 100 μm). Instrumented indentation was selected for characterization because it allows for small, precisely controlled testing areas. To ensure that bulk mechanical properties of samples were characterized, the indentation depth of the large tip was kept constant at 15 μm. This ensures any artificially stiff top layer was by-passed and the bulk sample was fully characterized.[35] Each ICN-M sample was tested along its length axis to characterize gradient formation.

Young's modulus results (Figure 3 A) illustrate that the highest stiffness for all ICN-M samples occur at the end of the sample which remained in the metal solution the longest, and that all samples display gradual stiffness decrease along their length axis. ICN-Zn displayed the highest stiffness for all tested samples at 108 ± 7 MPa (Table 1). Additionally, ICN-Zn possessed the largest and most gradually decreasing gradient span from 108 ± 7 to 0.59 ± 0.01 MPa. To the best of our knowledge, at over two orders of magnitude (230 fold increase), this stiffness gradient represents the largest continuous synthetic mechanical gradient made to date. In fact, this range in stiffness closely matches the magnitude of gradient observed in squid beaks, a benchmark for many gradient materials.[21] After ICN-Zn, ICN-Cu displayed the

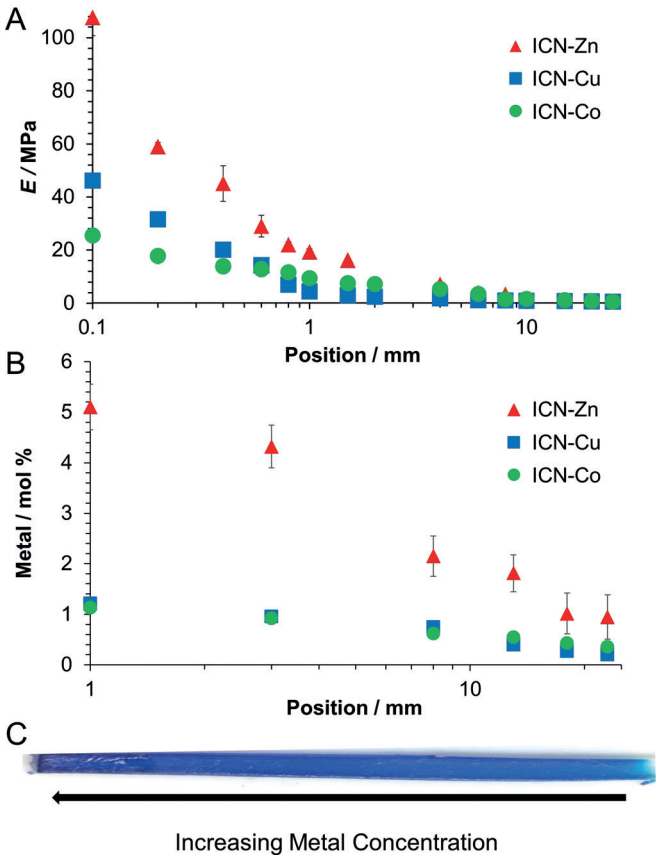

Figure 3. A) Gradient of Young's modulus (*E*) along the lateral axis of the samples as determined by instrumented indentation. B) Relative metal concentration (with respect to C, N, O) along the lateral axis of the samples as determined by XPS C) An image of the ICN-Cu sample.

Table 1: Minimal and maximal stiffness of each ICN material as determined by instrumented indentation.

Sample	Max. $E^{[a]}$	Min. $E^{[a]}$	Fold increase
ICN-Zn	108 ± 7	0.47 ± 0.01	230
ICN-Cu	46 ± 1	0.38 ± 0.01	121
ICN-Co	25 ± 2	0.34 ± 0.01	74

[a] Young's modulus (*E*) is measured in MPa via instrumented indentation.

next highest maximum stiffness (46 ± 1 MPa), followed by ICN-Co (25 ± 2 MPa) (Table 1). To confirm that the indentation data represent bulk mechanical properties, non-gradient bulk (Bulk-M) samples were prepared for tensile testing. Bulk-M samples with identical polymer composition and thickness were swelled with metal salt to mimic the stiffest end of gradient samples ([imidazole]/[M^{2+}] = 4.0). The data showed strong agreement between indentation and tensile measurements (Table S2), validating the use of indentation for testing the mechanical properties. Given the fact that the CGP fabrication method relies on metal infiltration from the surface to the center of samples, there is likely a gradient of mechanical properties through the thickness of the sample, which is hard to measure by either indentation or tensile technique. Nevertheless, the final result is a continuous gradient in bulk mechanical properties along the length axis. The local hardness of all specimens was also determined via instrumented indentation (Figure S3). In general, the observed hardness gradients spanned over one order of magnitude. Interestingly, ICN-Co displays the highest hardness of all samples, rather than ICN-Zn. This may be because Co–imidazole complexes exist as ML_6 species, while Zn–imidazole complexes exist as ML_4 complexes. This higher degree of crosslinks per metal atom could lead to a higher resistance to permanent shape change (i.e., hardness).

To confirm that the stiffness and hardness gradients were caused by the gradient of incorporated metal ions, X-ray photoelectron spectroscopy (XPS) was employed to determine relative metal concentrations along the lateral axis of the specimen. XPS was chosen because it can detect small metal concentrations, examine spatially distinct locations along the lateral axis, and is generally non-destructive to the sample. An argon gas cluster ion source (GCIS) was used to remove surface contaminants (Ar2000+, 5 keV). Region scans of the major atomic components (C, O, N) of the ICN were used to determine the relative abundance of the metal ions (Zn, Cu, Co) and confirm that the correct atomic ratios of elements were present for the ICN (see the Supporting Information for details of XPS determination). Indeed, along the lateral axis of the specimen, gradients of all 3 metals were observed (Figure 3B). ICN-Zn contains the largest relative percentage of metal (ranging from 0.9–5.1%, Table 2) while

Table 2: Minimal and maximal relative metal amount of each ICN material as determined by XPS.

Sample	Max. metal [mol%][a]	Min. metal [mol%][a]	Fold increase
ICN-Zn	5.1 ± 0.5	0.9 ± 0.4	5.7
ICN-Cu	1.21 ± 0.06	0.20 ± 0.02	6.1
ICN-Co	1.13 ± 0.07	0.35 ± 0.05	3.2

[a] Metal mol% was determined via XPS and is relative to the carbon, nitrogen and oxygen content of the polymer.

ICN-Cu and ICN-Co contain less relative metal (ranging from 0.20–1.21% and 0.35–1.13% respectively, Table 2). Determination of metal concentration closer than 1 mm from the edge of the sample was not possible due to signal interference from the sample holder. Due to the small penetration depth of XPS, energy-dispersive X-ray spectroscopy (SEM-EDX) spectra were obtained for ICN-Zn to confirm that the zinc salts could penetrate deep into the ICN sample. SEM-EDX measurements were performed on the surface and at the center of the cross-section at various locations along the length axis of the sample (Figure S4). SEM-EDX showed that metal concentration in ICN-Zn decreased by about 50% from the surface to the center, indicating that a gradient along the thickness of the sample has also been formed. Presumably, this gradient is formed due to the decreased mobility of metal ions within the polymer network. While this gradient along the thickness does not compromise the formation of gradient mechanical properties in bulk along the length axis, reduction of this effect should be feasible through further engineering controls.

The excellent correlation between the metal concentration gradient and the mechanical gradient observed implies that metal–imidazole interactions cause the strengthening of the material. The mechanical gradient is not linear, which is in line with our previous observation that mechanical properties do not depend linearly on metal to ligand ratio. In our previous study of similar Zn^{2+}–imidazole networks,[34] we observed relatively small mechanical changes for a large range of [imidazole]/[Zn^{2+}] ratio until it approaches ~4.0, when a dramatic increase in mechanical properties was observed. In our CGP sample preparation, we aimed to reach [imidazole]/[Zn^{2+}] ~ 4.0 at the end of the sample. The similar dramatic increase in Young's modulus in the very end of the sample suggests that the [imidazole]/[Zn^{2+}] approaches this critical value at the end of the sample. This roughly agrees with the XPS data. As an example, incorporation of the Zn^{2+} into the polymer at [imidazole]/[Zn^{2+}] ratio of 4.0 would give roughly 7.5 mol% Zn^{2+}. The maximal [Zn^{2+}] of 5.1 mol% measured in the bulk sample is close to this amount.

While the same metal concentrations for M-NTf solutions were used for all samples during swelling, the gradient behaviour for ICN-M samples differed based on metal selection. ICN-Zn formed a significantly larger gradient than both ICN-Cu and ICN-Co. This agrees with the XPS data, which demonstrates the ICN-Zn had higher metal incorporation across the lateral axis. While the exact reason for this is still unknown, we speculate that it is related to both the coordination geometry and ligand exchange kinetics for different metal–ligand complexes. While Zn^{2+} is known to form only ML_4 complexes with imidazole ligands, Co^{2+} and Cu^{2+} can form six coordinate species.[33,34] Additionally, the ligand exchange kinetics all differ between these metal complexes. Presumably, the higher coordination number and slower ligand exchange kinetics for Co^{2+} and Cu^{2+} hinder the metal uptake and affect network formation. Further studies are currently underway to understand the mechanism for the different behaviour.

In summary, the ICN-Zn network demonstrated in this work represents the largest continuous gradient span in mechanical properties observed to date at over 2 orders of magnitude, representing a dramatic improvement in gradient materials. In addition, using only a two-step synthesis and a common laboratory syringe pump, the ICN-M gradient materials can be reliably produced showing their broad appeal and ease of synthesis. We anticipate that introduction of these types of monodentate, metallopolymer gradients will spur further studies into the biomimetic, dissipative properties of these synthetic materials. With more rigorous engineering control (pull rate, temperature, metal added), we believe materials with much larger mechanical gradients and more homogeneous metal incorporation along the thickness axis could feasibly be obtained. In addition, the flexibility of this system will allow for a variety of different mechanical gradients to be studied using different metals, labile ligands, and/or counterions. Ongoing studies pursuing these goals, as well as gaining more mechanistic insight, are currently being undertaken in our lab.

Acknowledgements

We thank D. Mozhdehi for his helpful insights. This work was supported by the US Department of Energy, Division of Materials Sciences, under Award DE-FG02-04ER46162. N.J.O. was supported under award 5F31GM115077. Scanning electron microscopy and energy-dispersive X-ray spectroscopy work was performed at the UC Irvine Materials Research Institute (IMRI). XPS work was performed at the UC Irvine Materials Research Institute (IMRI) using instrumentation funded in part by the National Science Foundation Major Research Instrumentation Program under grant no. CHE01338173.

Conflict of interest

The authors declare no conflict of interest.

Keywords: bioinspired materials · gradient materials · mechanical properties · metallopolymers · polymers

How to cite: *Angew. Chem. Int. Ed.* **2017**, *56*, 15575–15579
Angew. Chem. **2017**, *129*, 15781–15785

[1] J. C. Weaver, G. W. Milliron, A. Miserez, K. Evans-Lutterodt, S. Herrera, I. Gallana, W. J. Mershon, B. Swanson, P. Zavattieri, E. DiMasi, et al., *Science* **2012**, *336*, 1275–1280.
[2] S. Suresh, *Science* **2001**, *292*, 2447–2451.
[3] R. Libanori, R. M. Erb, A. Reiser, H. Le Ferrand, M. J. Süess, R. Spolenak, A. R. Studart, *Nat. Commun.* **2012**, *3*, 1265.
[4] L. Ionov, *Mater. Today* **2014**, *17*, 494–503.
[5] K. U. Claussen, T. Scheibel, H.-W. Schmidt, R. Giesa, *Macromol. Mater. Eng.* **2012**, *297*, 938–957.
[6] K. U. Claussen, R. Giesa, H.-W. Schmidt, *Polymer* **2014**, *55*, 29–38.
[7] J. D. Fox, J. R. Capadona, P. D. Marasco, S. J. Rowan, *J. Am. Chem. Soc.* **2013**, *135*, 5167–5174.
[8] J. Kim, M. M. Mok, R. W. Sandoval, D. J. Woo, J. M. Torkelson, *Macromolecules* **2006**, *39*, 6152–6160.
[9] Y.-Q. Wang, Y. Wang, H.-F. Zhang, L.-Q. Zhang, *Macromol. Rapid Commun.* **2006**, *27*, 1162–1167.
[10] X. Zhang, P. Hassanzadeh, T. Miyake, J. Jin, M. Rolandi, *J. Mater. Chem. B* **2016**, *4*, 2273–2279.
[11] Z. Lin, X. Gui, Z. Zeng, B. Liang, W. Chen, M. Liu, Y. Zhu, A. Cao, Z. Tang, *Adv. Funct. Mater.* **2015**, *25*, 7173–7179.
[12] B. Wang, A. J. Benitez, F. Lossada, R. Merindol, A. Walther, *Angew. Chem. Int. Ed.* **2016**, *55*, 5966–5970; *Angew. Chem.* **2016**, *128*, 6070–6074.
[13] D. Wang, H. Zhang, J. Guo, B. Cheng, Y. Cao, S. Lu, N. Zhao, J. Xu, *Macromol. Rapid Commun.* **2016**, *37*, 655–661.
[14] L. V. Karabanova, S. V. Mikhalovsky, A. W. Lloyd, G. Boiteux, L. M. Sergeeva, T. I. Novikova, E. D. Lutsyk, S. Meikle, *J. Mater. Chem.* **2005**, *15*, 499.
[15] C. L. Qin, D. Y. Zhao, X. D. Bai, X. G. Zhang, B. Zhang, Z. Jin, H. J. Niu, *Mater. Chem. Phys.* **2006**, *97*, 517–524.
[16] A. Ahmed, J. Smith, H. Zhang, *Chem. Commun.* **2011**, *47*, 11754.
[17] X. Li, M. R. MacEwan, J. Xie, D. Siewe, X. Yuan, Y. Xia, *Adv. Funct. Mater.* **2010**, *20*, 1632–1637.
[18] J. V. Karpiak, Y. Ner, A. Almutairi, *Adv. Mater.* **2012**, *24*, 1466–1470.
[19] L. Yang, G. Zhang, N. Zheng, Q. Zhao, T. Xie, *Angew. Chem. Int. Ed.* **2017**, *56*, 12599–12602; *Angew. Chem.* **2017**, 129, 12773–12776.

[20] H. Chai, J. J.-W. Lee, P. J. Constantino, P. W. Lucas, B. R. Lawn, *Proc. Natl. Acad. Sci. USA* **2009**, *106*, 7289 – 7293.
[21] A. Miserez, T. Schneberk, C. Sun, F. W. Zok, J. H. Waite, *Science* **2008**, *319*, 1816 – 1819.
[22] S. F. Fischer, M. Thielen, R. R. Loprang, R. Seidel, C. Fleck, T. Speck, A. Bührig-Polaczek, *Adv. Eng. Mater.* **2010**, *12*, B658 – B663.
[23] M. Ruggeberg, I. Burgert, T. Speck, *J. R. Soc. Interface* **2010**, *7*, 499 – 506.
[24] M. J. Harrington, J. H. Waite, *Adv. Mater.* **2009**, *21*, 440 – 444.
[25] X. Li, J. Xie, J. Lipner, X. Yuan, S. Thomopoulos, Y. Xia, *Nano Lett.* **2009**, *9*, 2763 – 2768.
[26] H. A. Lowenstam, S. Weiner, *On Biomineralization*, Oxford University Press, Oxford, **1989**.
[27] H. A. Lowenstam, *Science* **1967**, *156*, 1373 – 1375.
[28] J. D. Currey, *J. Exp. Biol.* **1999**, *202*, 3285 – 3294.
[29] H. C. Lichtenegger, T. Schoberl, M. H. Bartl, H. Waite, G. D. Stucky, *Science* **2002**, *298*, 389 – 392.
[30] H. C. Lichtenegger, T. Schoberl, J. T. Ruokolainen, J. O. Cross, S. M. Heald, H. Birkedal, J. H. Waite, G. D. Stucky, *Proc. Natl. Acad. Sci. USA* **2003**, *100*, 9144 – 9149.
[31] J. H. Waite, H. C. Lichtenegger, G. D. Stucky, P. Hansma, *Biochemistry* **2004**, *43*, 7653 – 7662.
[32] R. K. Khan, P. K. Stoimenov, T. E. Mates, J. H. Waite, G. D. Stucky, *Langmuir* **2006**, *22*, 8465 – 8471.
[33] D. Mozhdehi, S. Ayala, O. R. Cromwell, Z. Guan, *J. Am. Chem. Soc.* **2014**, *136*, 16128 – 16131.
[34] D. Mozhdehi, J. A. Neal, S. C. Grindy, Y. Cordeau, S. Ayala, N. Holten-Andersen, Z. Guan, *Macromolecules* **2016**, *49*, 6310 – 6321.
[35] A. C. Fischer-Cripps, *Nanoindentation*, Springer New York, New York, **2011**.

Manuscript received: July 25, 2017
Accepted manuscript online: October 9, 2017
Version of record online: November 7, 2017

